Kagome network compounds and their novel magnetic properties

Swapan K. Pati*[a] and C. N. R. Rao*[b]

Received (in Cambridge, UK) 29th April 2008, Accepted 19th June 2008
First published as an Advance Article on the web 27th August 2008
DOI: 10.1039/b807207h

Compounds possessing the Kagome network are truly interesting because of their unusual low-energy properties. They exhibit magnetic frustration because of the triangular lattice inherent to the hexagonal bronze structure they possess, as indeed demonstrated by some of the Fe^{3+} jarosites, but this is not the general case. Kagome compounds formed by transition metal ions with varying spins exhibit novel magnetic properties, some even showing evidence for magnetic order and absence of frustration. We describe the structure and magnetic properties of this interesting class of materials and attempt to provide an explanation for the variety of properties on the basis of theoretical considerations.

1. Introduction

Kagome is a Japanese word meaning *hole in the basket* and metal compounds possessing the hexagonal bronze structure with a triangular lattice are referred to as Kagome network compounds. Many transition metal compounds with Kagome networks have been synthesized and characterized in recent years. One of the most important characteristics of the Kagome network compounds, as typified by the Fe^{3+} jarosites, is magnetic frustration.

Frustration is an old topic that can be traced back to the work of Linus Pauling and others on the frozen disorder of crystalline ice.[1–3] Frustration arises when the geometry of a system allows for a set of degenerate ground states. In the case of ice, this corresponds to the different ways of orienting the water molecules without changing the energy of the system. Such a ground state entropy in ice was observed experimentally.[2,3] The same approach can be extended to antiferromagnetically coupled tetrahedra, or systems with triangular symmetry which show a rich manifestation of magnetic frustration.[4–9]

Frustration has a geometrical origin wherein a set of degrees of freedom becomes incompatible with the extended symmetry of the system. A good example is the impossibility of close-packing pentagons in two-dimensional space. The under-constraint of a lattice geometry to the number of independent constraints of local geometry gives rise to geometrical frustration. In magnetic systems, this results in certain unique low energy characteristics in the magnetic properties and thus has generated tremendous interest.[10–15] Examples of geometrically frustrated magnetic systems include one-dimensional zigzag, ladder, and sawtooth lattice structures, two-dimensional layered, triangular and Kagome lattices and three dimensional pyrochlore lattice systems.[16–26] In all these systems, geometrical frustration is manifested due to the competition of the antiferromagnetic interactions between the neighboring spins.

The propensity to adopt many unusual magnetic structures is mostly found in two-dimensional frustrated lattice systems, the Kagome and the triangular lattices. While the triangular lattice point has six nearest neighbors and the adjacent triangles share one side or two lattice points, the Kagome lattice point has four nearest neighbors with the adjacent triangles on the lattice sharing only one lattice point. If the interactions are

[a] *Theoretical Sciences Unit, Jawaharlal Nehru Center for Advanced Scientific Research, Bangalore 560064, India. E-mail: pati@jncasr.ac.in; Fax: +91 80 22082767; Tel: +91 80 22082839; http://www.jncasr.ac.in/pati/*
[b] *Chemistry and Physics of Materials Unit, Jawaharlal Nehru Center for Advanced Scientific Research, Bangalore 560064, India. E-mail: cnrrao@jncasr.ac.in; Fax: +91 80 22082760; Tel: +91 80 22082761*

Swapan K. Pati

Swapan K. Pati obtained his PhD from the Indian Institute of Science, Bangalore, followed by postdoctoral work at University of California and Northwestern University. He is currently an Associate Professor at the Jawaharlal Nehru Centre for Advanced Scientific Research. His research interests include quantum magnetism and developing new theoretical tools for a holistic understanding of structure–property correlations.

C. N. R. Rao

C. N. R. Rao obtained his PhD from Purdue University and DSc degree from the University of Mysore. He is the National Research Professor of India, Linus Pauling Research Professor at the Jawaharlal Nehru Centre for Advanced Scientific Research and Honorary Professor at the Indian Institute of Science and a member of several academies. His research interests are in the chemistry of materials.

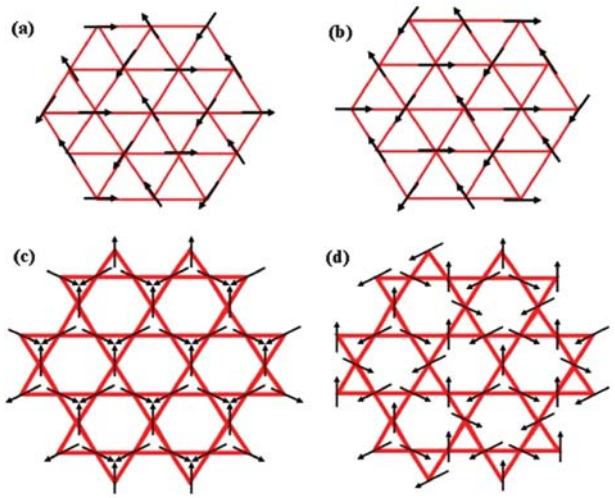

Fig. 1 Two degenerate ground state structures of an antiferromagnetically coupled triangular lattice (a and b). Kagome lattice with two spin orientations: $Q = 0$ (c) and $Q = \sqrt{3} \times \sqrt{3}$ (d).

considered to be nearest neighbor antiferromagnetic within the Heisenberg model, for a lattice with triangular symmetry frustration would simply lead to a 120° array of spin configurations, as shown in Fig. 1a. Such a state will be doubly degenerate (Fig. 1b) associated with the handedness or chirality of the vector array, in addition to the trivial degeneracy associated with the global rotation of spins. Since this configuration may be extended infinitely in the plane of the paper in a unique fashion to produce a long-range ordered spin array, the ground state and excitations are believed to be rather conventional.[27]

When the triangular plaquettes are connected through corner sharing vertices to form the Kagome lattice, the order within an isolated plaquette cannot be propagated in an unambiguous fashion. Fig. 1c and d display two of the many manifolds of possible spin states which satisfy the requirement that all spins are at 120° to each other, the so-called $Q = 0$ state (Fig. 1c) and the $Q = \sqrt{3} \times \sqrt{3}$ state (Fig. 1d), where Q corresponds to the wave vector. If thermal or quantum fluctuations are considered, it is possible that a subset of the manifold of ground states would be selected. For classical (large) spins, small quantum or thermal fluctuations would select spin configurations in which all the spins are coplanar and possibly at $T = 0$ it adopts the structure shown in Fig. 1d. Interestingly, there is also a strong link between Kagome systems with frustration and hole-doped high T_c cuprate materials. In both cases, the number of nearest neighbors is the same (4) and the hole doping becomes equivalent to ground state degeneracy due to magnetic frustration.[26] The research efforts in this area are, therefore, highly interdisciplinary as one would expect.

With such a variety of magnetic ground state structures, the Kagome system offers new, interesting and exotic possibilities of low-energy and low-temperature properties. Thus, the Kagome lattice has emerged to be a classical case of a Heisenberg antiferromagnet which could represent a quantum spin liquid phase and offers the possibility of exploring both classical and quantum spin ground and excited states together with the correlated electron problems.

There has been a large number of theoretical and experimental studies recently on the various aspects of magnetic frustration in a large class of Kagome systems.[20–24] Although the ideal Kagome lattice compounds synthesized so far are only a few, there have been many efforts to synthesize and characterize different types of Kagome structures in the past few years. For example, there exist Kagome systems varying from $Rb_2M_3S_4$[28–31] (M is a magnetic ion such as Ni, Co, Mn) to $NaFe_3(SeO_4)_2(OH)_6$,[32] magnetoplumbite $SrCr_xGa_{12-x}O_{19}$,[33] staircase $M_3V_2O_8$ (M is a magnetic ion),[34] spherical Keplerates[35] and jarosites with formula $AM_3(OH)_6(SO_4)_2$.[6,24,25] Besides these, the spin lattices in $La_4Cu_3MoO_{12}$[36] and $RCuO_{2.66}$[37] are reported to be identical with the Kagome lattice. Two-dimensional solid ^{3}He adsorbed on graphite has also been studied as a Kagome antiferromagnetic system.[38] Although all these materials belong to the family of Kagome systems, it will be beyond the scope of this *feature article* to discuss all the structures. The Kagome staircase structure, however, is different in that the layers are not two-dimensional but are buckled in and out of the plane. We shall concentrate more on the Kagome network compounds of different ions possessing different site spins.

Theoretically, the ideal $S = \frac{1}{2}$ Kagome lattice antiferromagnet has been studied extensively. Studies based on the exact diagonalization of finite systems and series expansions[39–41] suggest that the system has a quantum disordered ground state. Finite size studies show a gap to spin excitations, but the most fascinating aspect of these numerical studies is the existence of a large number of singlet excitations below the lowest triplet state. Their number appears to grow exponentially with the size of the system.[42,43] Although there exist volumes of theoretical work on Kagome lattices, most of these are restricted to $S = \frac{1}{2}$ Kagome systems. We have recently attempted to explain the magnetic properties of Kagome systems on the basis of the magnitude of spins.[44]

In this *feature article*, we discuss the structures and magnetic properties of a number of Kagome systems synthesized with several transition metal ions such as Fe^{3+}, Cu^{2+}, Mn^{2+}, V^{3+}, Co^{2+}, Fe^{2+}, Ni^{2+} and a Fe^{2+}/Fe^{3+} mixed valent complex. We then try to rationalize the observation on magnetic properties in the jarosite class of materials based on theoretical analysis. We conclude with a summary and future outlook.

2. Experimental scenario

There has been much progress in the synthesis of the jarosite class of compounds, with the general formula $AM_3(OH)_6(XO_4)_2$. The A site is usually occupied by a monovalent, divalent or a trivalent cationic species which has a coordination number greater or equal to nine. The M site is the metal site in an octahedral coordination and the X site is occupied by a P^{5+}, As^{5+} or S^{6+} in a tetrahedral oxygen environment. The layered Kagome hexagonal sheets are separated by the A cations.[6] In general, the corner-shared tetrahedral lattice, which occurs in both spinel and pyrochlore structure materials, is called the pyrochlore lattice. For planar lattices, the mode of stacking in three dimensions of edge-shared triangular sheets with ···ABCABC··· stacking of Kagome

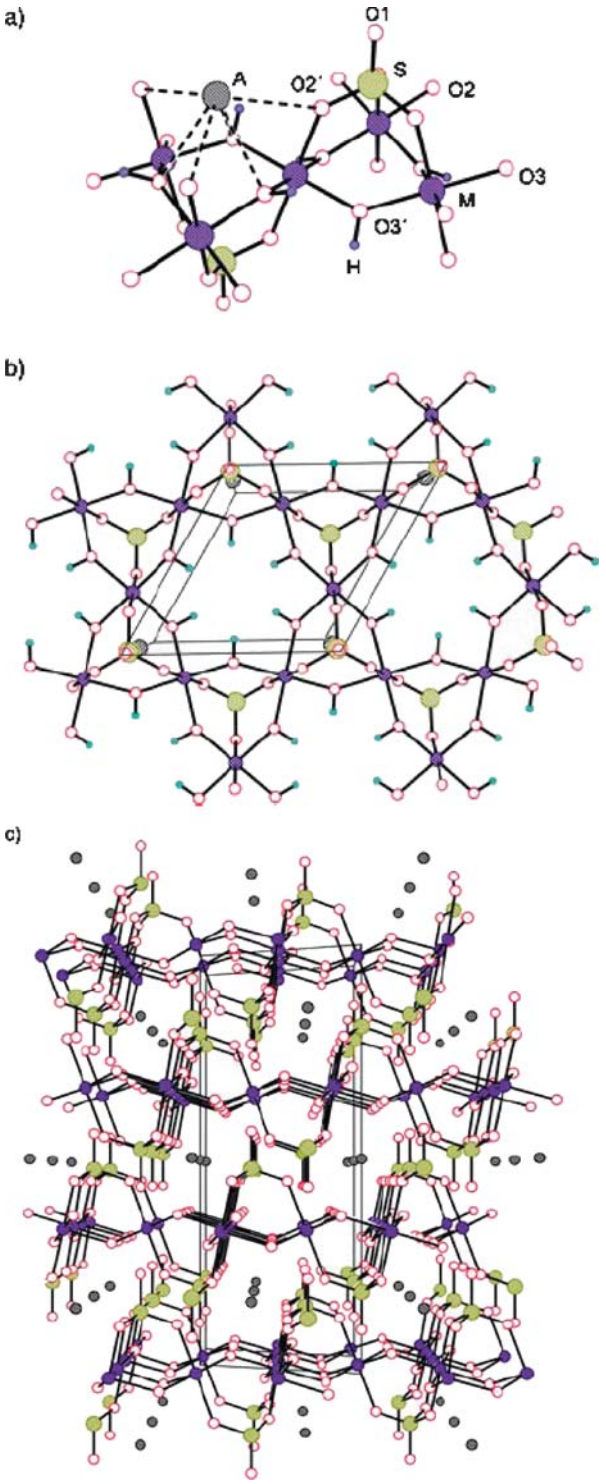

Fig. 2 The X-ray crystal structure of (a) the magnetic subunit of $Fe_3(\mu\text{-}OH)_3$ triangles; (b) the in-plane segment of the Kagome layer; and (c) a side-view of stacked Kagome layers. In (a) the sphere coding of the atoms is presented.[25]

layers yields the pyrochlore lattice, as shown Fig. 2. The elementary triangles in the two-dimensional sheet are capped by the XO_4 tetrahedra which are positioned above and below the sheet in alternate fashion (see Fig. 2). The magnetic ion at each of the vertices of the triangular array, with four neighbors, confers unusual correlated magnetic properties.[45]

Jarosite-type materials are difficult to obtain in pure single crystal form, but highly stoichiometric and pure samples are essential to obtain consistent and meaningful results. Intense research in the past decade has sought to develop a few new synthetic routes for the preparation of pure and highly crystalline samples without many defects or with almost full coverage. While redox-based techniques have been employed by Nocera's group to prepare single crystalline Kagome samples with almost full coverage of the magnetic ions, many organically templated Kagome compounds have been synthesized by hydrothermal techniques by us. The employment of new synthetic routes has resulted in a large class of new materials. For example, a class of Kagome materials with the general formula $MCu_3(OH)_6Cl_2$ with various metal (M) ions has recently been prepared.[46,47] It has also been possible to prepare Kagome compounds with two different metals or the same metal with two different oxidation states.[48] Depending on the charge imbalance of the metal ions and the preparatory conditions, the resultant compounds exhibit different crystal symmetries and chemical formulae. The magnetic properties of these materials have been investigated after establishing the structures by X-ray crystallography together with compositional analysis and spectroscopic data.[49–55]

2.1 $S = \frac{5}{2}$ Kagome compounds

The alunite superfamily subgroup, with composition $KFe_3(SO_4)_2(OH)_6$, show layered Kagome network features. The crystal structure consists of $Fe_3^{III}(\mu\text{-}OH)_3$ triangles (Fig. 2a), capped by sulfate anions positioned alternately up and down about a hexagonal network forming the Kagome layers (Fig. 2). To date, there has been much progress with new redox based methods, and synthesis of Fe jarosites with general formula $AFe_3(OX)_6(TO_4)_2$ featuring different cations and anionic groups ($A = Na^+$, K^+, Rb^+, NH_4^+, $\frac{1}{2}Pb^{2+}$, Ag^+, Tl^+ and $TO_4 = SO_4^{2-}$ and $(OX)_6 = (OH)_6$ and $(OD)_6$; $A = K^+$ and Rb^+ and $TO_4 = SeO_4^{2-}$ and $(OX)_6 = (OH)_6$) with almost complete coverage has been possible.[45,56–62] In the crystal, while the FeO_6 octahedra are clearly puckered, the Fe ions form a perfectly planar Kagome net. The layer stacking sequence is $\cdots$ABCABC$\cdots$ along the *c*-axis, shown in Fig. 2. The magnetic properties of these materials are very interesting (see Fig. 3). Except for $(D_3O)Fe_3(SO_4)_2(OD)_6$, which shows no long range order[63,64] down to 1.5 K (although there exists an apparent transition at 13.8 K), all the other Fe jarosites show long range magnetic ordering with a very large negative Curie–Weiss constant (θ) value, even with 90% coverage of the Kagome net.[45,61,62] In Table 1, the Curie–Weiss constant and ordering temperature are listed for a number of these Fe^{3+} jarosite compounds.

There have been attempts to synthesize Kagome compounds with $S = \frac{5}{2}$ with a transition metal ion other than Fe^{3+}. One such system synthesized is an amine templated manganese(II) sulfate of the composition $[C_4N_2H_{12}][NH_4]_2[Mn_3^{II}F_6(SO_4)_2]$, with the Kagome structure, under solvothermal conditions.[65] The structure consists of vertex-sharing $Mn^{II}F_4O_2$ octahedra

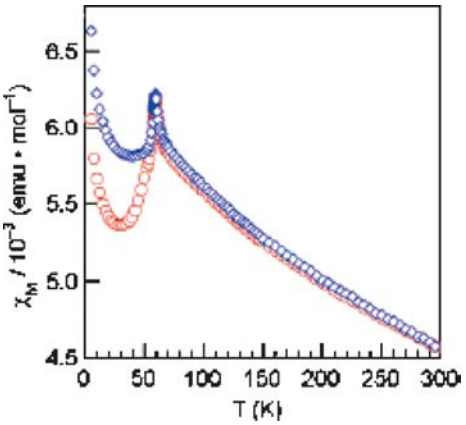

Fig. 3 Field-cooled (FC, ◇) and zero-field-cooled (ZFC, ○) susceptibilities for $AgFe_3(OH)_6(SO_4)_2$ at a 100 Oe measuring field.[45]

and SO_4 tetrahedral units, which are fused together by Mn–F–Mn and Mn–O–S bonds. The distorted octahedron around Mn^{2+} has the oxygen atoms from the sulfate along the *z*-axis and the F atoms along the *xy*-plane (Fig. 4). The magnetic properties of this compound differ from those of Fe^{3+} jarosites. Down to very low temperature, the magnetic susceptibility does not show any magnetic ordering while the θ value is found to be negative (−30 K).

2.2 $S = \frac{1}{2}$ Kagome compounds

Nocera *et al.* have hydrothermally synthesized a series of compounds of general formula $Zn_xCu_{4-x}(OH)_6Cl_2$ with $0 < x < 1$, with variable Cu/Zn composition.[46,47] The crystal symmetry depends crucially on the *x* value; for $x < 0.33$, the crystal symmetry is monoclinic with distorted Kagome lattice and for $x > 0.33$, the crystal symmetry increases to rhombohedral, with equilateral Cu triangular plaquettes. The magnetic measurements for the series with variance of *x* show that for $x = 0$, there exists a ferromagnetic transition at $T_c = 6.5$ K and as *x* increases from 0, the ferromagnetic transition is maintained, but the corresponding T_c decreases (Fig. 5). For $x = 1$, *i.e.*, at full Zn^{II} occupancy, no magnetic ordering has been observed. The Curie–Weiss constant is found to be large and negative and its magnitude decreases with an increase in *x*, as expected.

Table 1 Curie–Weiss constants (θ_c in K) and antiferromagnetic ordering temperatures (T_0 in K) for various Fe^{3+} jarosites

Compound	θ_c/K	T_0/K
$(H_3O)Fe(SO_4)_2(OH)_6$	−820	65
$(D_3O)Fe_3(SO_4)_2(OD)_6$	−700	—
$(ND_4)Fe_3(SO_4)_2(OD)_6$	−640	46
$NaFe_3(SO_4)_2(OD)_6$	−667	42
$RbFe_3(SO_4)_2(OD)_6$	−688	47
$KFe_3(SO_4)_2(OD)_6$	−600	46
$AgFe_3(SO_4)_2(OD)_6$	−677	51
$NaFe_3(SO_4)_2(OH)_6$	−825	61.5
$RbFe_3(SO_4)_2(OH)_6$	−829	64.5
$KFe_3(SO_4)_2(OH)_6$	−828	65.5
$AgFe_3(SO_4)_2(OH)_6$	−798	59.5
$TlFe_3(SO_4)_2(OH)_6$	−838	63.5
$Pb_{0.5}Fe_3(SO_4)_2(OH)_6$	−818	56.5

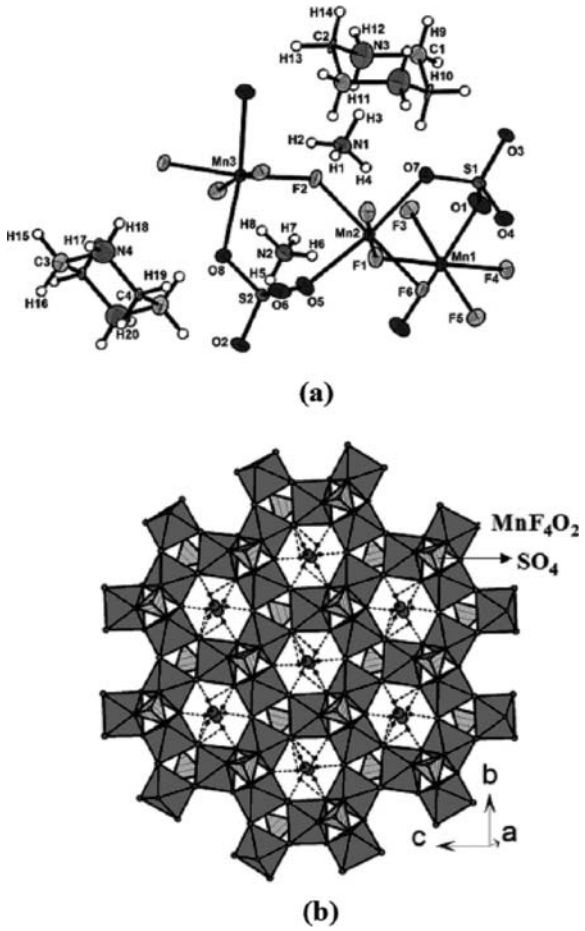

Fig. 4 (a) Labeled asymmetric unit of $[C_4N_2H_{12}][NH_4]_2[Mn^{II}_3F_6(SO_4)_2]$. Thermal ellipsoids are given at 50% probability. (b) Polyhedral view of the hexagonal Kagome layer. Note the presence of the ammonium ion in the hexagonal channel.[65]

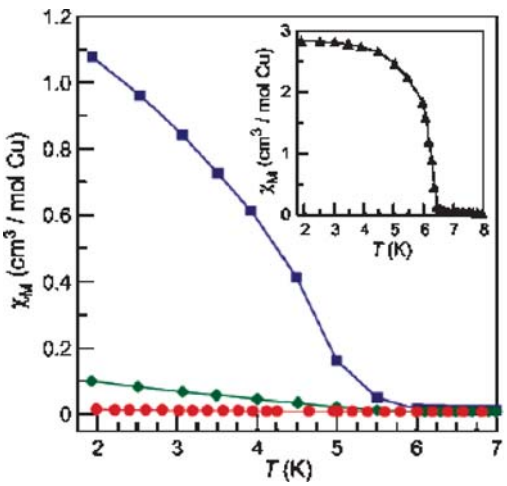

Fig. 5 (a) Low temperature dependence of χ_M for compounds with formula $Zn_xCu_{4-x}(OH)_6Cl_2$ for $x = 0$ (▲), 0.50 (■), 0.66 (◆) and 1.00 (●) as measured under ZFC conditions at 100 Oe (χ_M in the inset is for $x = 0$).[46]

2.3 $S = 1$ Kagome compounds

Recently, a phase-pure compound of the formula $[C_6N_2H_8][NH_4]_2[Ni_3F_6(SO_4)_2]$, was prepared under solvothermal conditions, where the magnetic ion Ni(II) is in the $S = 1$ state.[66]

The structure of this compound (Fig. 6a) consists of anionic layers of vertex-sharing $Ni^{II}F_4O_2$ octahedra and SO_4 tetrahedra fused together by Ni–F–Ni and Ni–O–S bonds. Each NiF_4O_2 unit shares four of its Ni–F vertices with similar neighbors, with the Ni–F–Ni bonds roughly aligned in the *ab*-plane. The Ni–O bond is canted from the *ab*-plane, which forces a three ring trio of apical Ni–O bonds closer together to allow them to be capped by the SO_4 tetrahedra. The sulfate groups are positioned alternately up and down about the hexagonal network. The three- and six-membered rings formed by the octahedra give rise to the in-plane connectivity of the hexagonal tungsten bronze sheets, characteristic of the Kagome lattice, as shown in Fig. 6b. The $[Ni_3F_6(SO_4)_2]^{4-}$ framework is balanced by the presence of protonated amine and NH_4^+ ions in the interlayer space and hexagonal channels, respectively. Magnetic measurements show that the

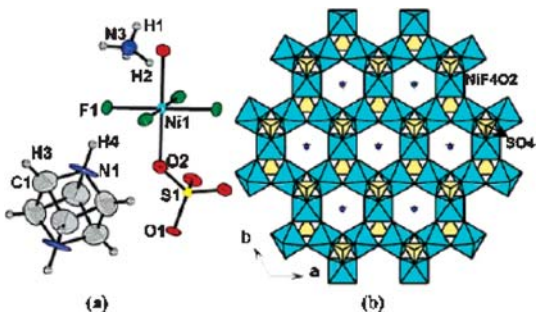

Fig. 6 (a) Labeled asymmetric unit of $[C_6N_2H_8][NH_4]_2[Ni_3F_6(SO_4)_2]$. Thermal ellipsoids are given at 50% probability. (b) Polyhedral view of the hexagonal Kagome layer. Note the presence of the ammonium ion in the hexagonal channel.[66]

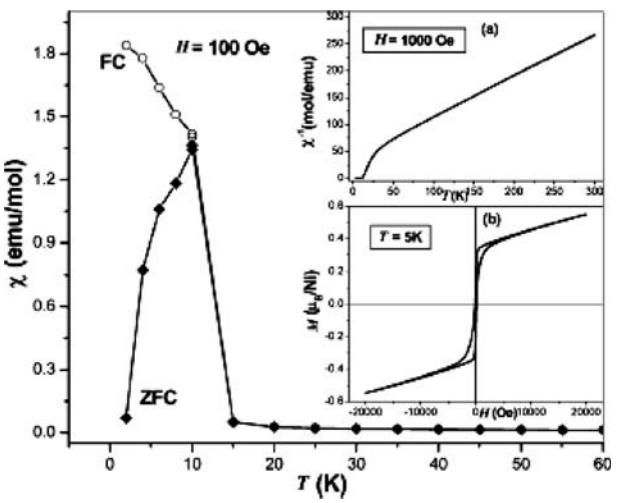

Fig. 7 Temperature dependence of the magnetic susceptibility of the Ni Kagome compound (100 Oe) under FC and ZFC conditions. Inset (a) shows the temperature variation of the inverse susceptibility at 1000 Oe. Inset (b) shows magnetic hysteresis at 5 K.[66]

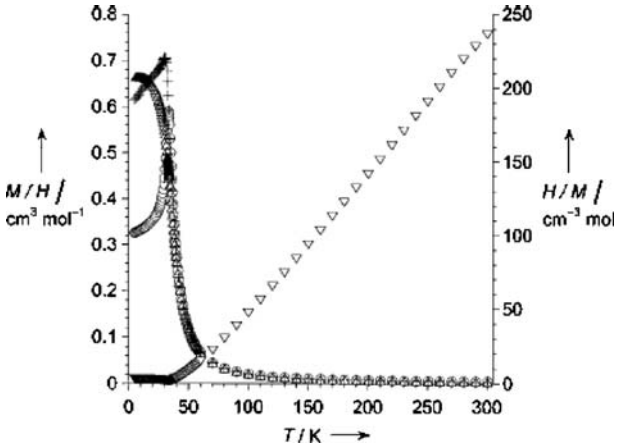

Fig. 8 Temperature dependence of M/H per mole of vanadium atoms for $NaV_3(OH)_6(SO_4)_2$ at applied magnetic field strengths of 0.5 (●), 5.0 (+), and 10.0 (△) kOe. The H/M *versus* T plot (▽) was measured at an applied field of 0.5 kOe.[68]

Curie–Weiss θ value is antiferromagnetic (−60 K), and the low-temperature magnetization data show hysteresis, possibly due to canted antiferromagnetic ordering (Fig. 7).[67]

There also exists an earlier example of a spin-1 Kagome lattice system with formula $NaV_3(OH)_6(SO_4)_2$, which was synthesized hydrothermally by Nocera *et al.*[68,69] The compound crystallizes in the rhombohedral space group $R\bar{3}m$, in which the vanadium ion is in the 3+ state and resides in a distorted octahedron, composed of four equatorial oxygen atoms from the bridging hydroxy groups and two axial oxygen atoms from the capping sulfate groups. Such a vanadium pseudo-octahedron is tetragonally elongated along its *z*-axis. The magnetic properties are found to depend crucially on the interlayer couplings (Fig. 8). The Curie–Weiss constant (θ) is found to be +53 K, which indicates that the intralayer coupling between vanadium centers is strongly ferromagnetic, with $T_c = 33$ K. From the magnetic field dependent susceptibility data, it has been concluded that the interlayer coupling is weakly antiferromagnetic.

2.4 $S = \frac{3}{2}$ Kagome compounds

An organically templated cobalt(II) sulfate of the composition, $[H_2N(CH_2)_4NH_2][NH_4]^{2-}[Co_3^{II}F_6(SO_4)_2]$, with the Kagome lattice was isolated by Rao *et al.*[70] The structure consists of anionic layers of vertex-sharing $Co^{II}F_4O_2$ octahedra and tetrahedral SO_4 units, which are fused together by Co–F–Co and Co–O–S bonds. Each CoF_4O_2 unit shares four of its Co–F vertices with similar neighbors, with the Co–F–Co bonds roughly aligned in the *bc*-plane. The Co–O bond is canted from the *bc*-plane and the Co–O vertex forces a three-ring trio of apical Co–O bonds closer together to allow them to be capped by the SO_4 tetrahedra. The three- and six-membered rings of octahedra from the in-plane connectivity are shown in Fig. 9. The magnetic measurements give a θ value of −35.5 K and an effective magnetic moment of 5.2 μ_B per Co from the Curie–Weiss fit, which is a little higher than the spin-only value due to orbital contributions as found in many other Co^{2+} compounds.[71]

There also exists another type of $S = \frac{3}{2}$ compound, the layered garnets $SrCr_xGa_{12-x}O_{19}$ (SCGO), which have been

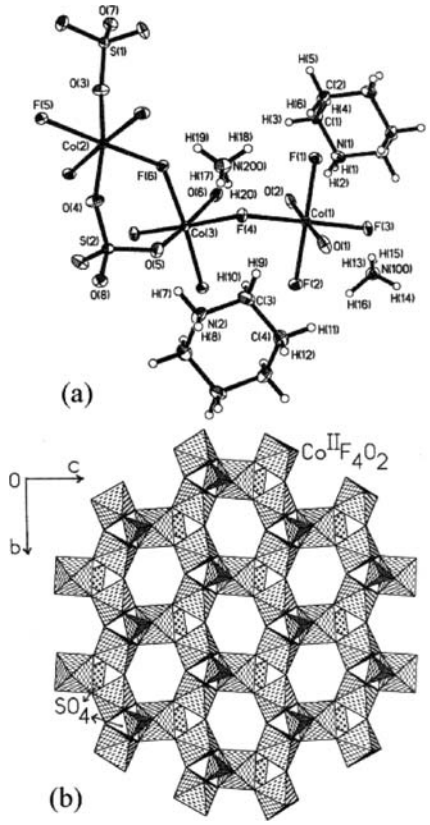

Fig. 9 (a) Asymmetric unit of $[H_2N(CH_2)_4NH_2][NH_4]^{2-}[Co^{II}_3F_6(SO_4)_2]$ (b) Polyhedral view of the Kagome layer.[70]

investigated quite extensively.[72–76] However, these materials contain an additional edge-sharing triangular (non-Kagome) lattice interposed between Kagome layers.

2.5 $S = 2$ Kagome compounds

A compound with the formula $[H_3N(CH_2)_6NH_3][Fe^{II}_{1.5}F_3(SO_4)]\cdot 0.5H_2O$ has been synthesized hydrothermally, where the magnetic ion is in the +2 state with integer spin.[77] The structure consists of anionic layers of vertex-sharing $Fe^{II}F_4O_2$ octahedra and tetrahedral SO_4 units, which are fused together by Fe–F–Fe and Fe–O–S bonds. Each FeF_4O_2 unit shares four of its Fe–F vertexes with similar neighbors, with the Fe–F–Fe bonds nearly aligned in the *ab*-plane. The Fe–O bond is canted from the *ab*-plane and the Fe–O vertex effectively forces a three-ring trio of apical Fe–O bonds closer together to allow them to be capped by the SO_4 tetrahedra. The three- and six-membered rings of octahedra, resulting from the in-plane connectivity, are shown in Fig. 10. Interestingly, the magnetic measurements show a magnetic polarization at low temperature reminiscent of ferrimagnetic ordering. The Curie–Weiss constant is found to be −70 K.

However, with a different set of initial conditions, a monophasic pale yellowish needle shaped crystal of an iron compound with the formula $[H_3N(CH_2)_2NH_2(CH_2)_2NH_2(CH_2)_2NH_3][Fe^{II}_3F_6(SO_4)_2]$, has been isolated.[78] In this system, there are five crystallographically distinct Fe atoms and two S atoms with all the Fe atoms having octahedral geometry. The Fe atoms have fluorine and oxygen neighbors to form FeF_4O_2

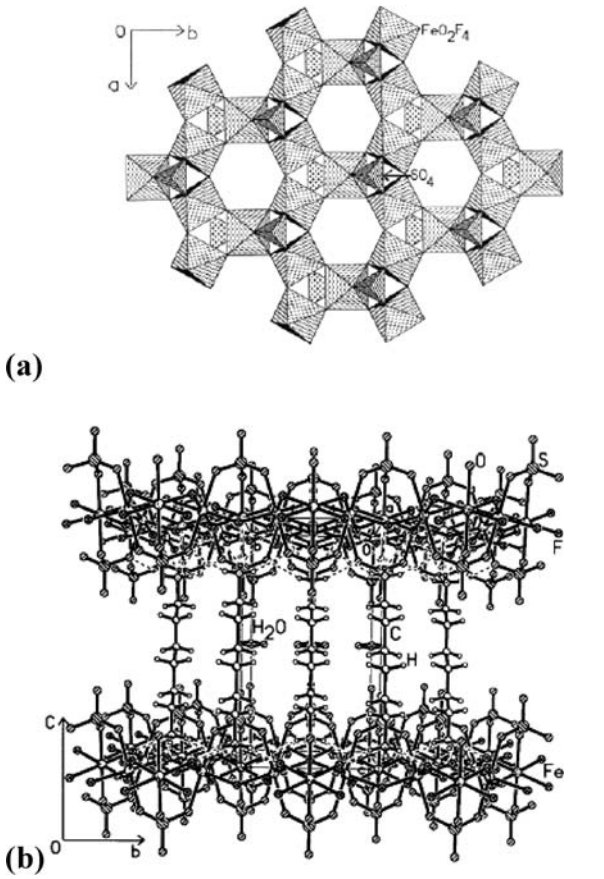

Fig. 10 The polyhedral view of $[H_3N(CH_2)_6NH_3][Fe^{II}_{1.5}F_3(SO_4)]\cdot 0.5H_2O$. The three-membered apertures are capped by sulfate moieties. (b) View along the *a*-axis showing the stacking of the layers pillared by the amine. The dotted lines indicate H-bond interactions.[77]

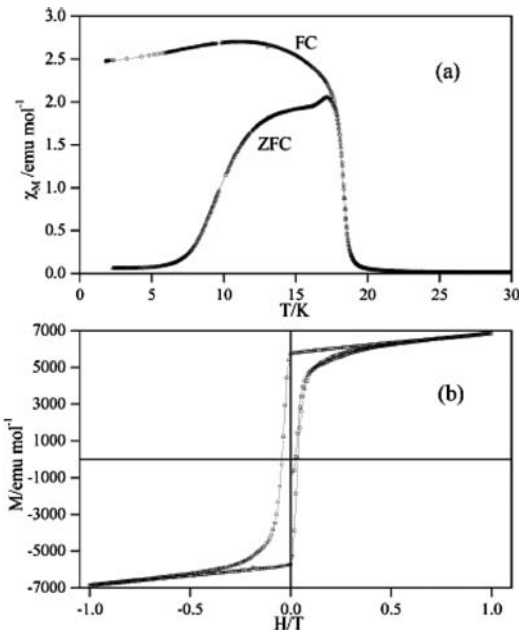

Fig. 11 (a) DC susceptibility data showing divergence between the ZFC and FC (at 100 Oe) behaviours. (b) Magnetic hysteresis at 10 K.[78]

octahedra. The structure consists of anionic framework layers of $[Fe_3F_6(SO_4)_2]$. Due to the presence of 50% edge-sharing octahedra, two types of triangular lattices are created. One type of three-ring trio is formed by the vertex-sharing of the FeF_4O_2 octahedra, creating a perfect three-membered ring, which is capped by the sulfate tetrahedron, as in a jarosite. On the other hand, the three-ring trio formed by two edge-sharing and one corner-sharing octahedra, creates a distorted triangular lattice which is bridged by the sulfate tetrahedron. This compound shows magnetic hysteresis (Fig. 11) below a critical temperature (18 K) due to the distortion caused by the presence of the edge sharing octahedra.

2.6 Mixed-valent iron Kagome compounds

In the process of finding new Kagome materials, a mixed-valent compound, $[HN(CH_2)_6NH][Fe^{III}Fe^{II}_2F_6(SO_4)_2]\cdot[H_3O]$, was synthesised by solvothermal methods.[48] The structure consists of anionic layers of corner sharing $Fe^{III}F_4O_2$ and $Fe^{II}F_4O_2$ octahedra and SO_4 tetrahedra. In Fig. 12, we show the structure of the compound to demonstrate how the Kagome lattice is derived from three and six-membered rings of octahedra, giving rise to the hexagonal tungsten-bronze-type sheets. There is 100% occupation, rendered possible by the presence of fluoride instead of the OH groups normally found in jarosites. The presence of the Fe^{II} and Fe^{III} states in the ratio 2 : 1 is consistent with the formula derived from crystallography and chemical analysis. Interestingly, the magnetic measurements show hysteresis at 10 K, however, the hysteresis data show a step-like behavior and a metamagnetic transition, the field required for the transition depending on the temperature.

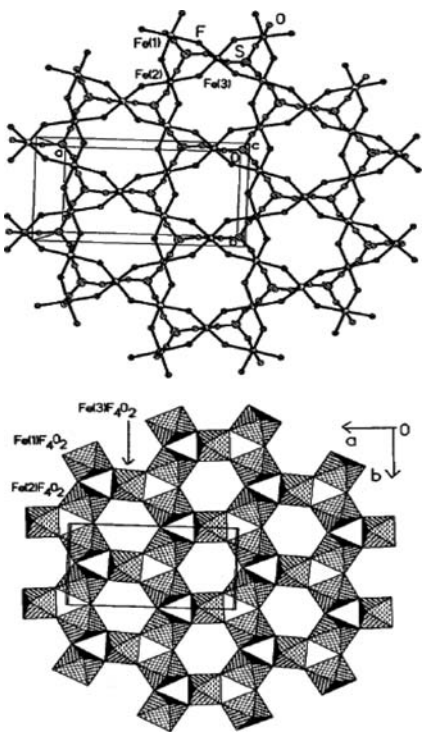

Fig. 12 (a) Ball and stick representation of a section of $FeFe_2F_6(SO_4)_2$, showing the presence of three- and six-membered rings, where the three rings are capped by sulfate tetrahedra. (b) Polyhedral view of the 2D network of corner sharing iron octahedra in the mixed valent compound in the *ab*-plane. Here Fe(1) and Fe(2) are in the +2 state and Fe(3) is in the +3 state.[48]

3. Approaches to understand frustration and related magnetic properties

As can be seen, experimental magnetic behavior varies considerably depending on the magnetic ions present and on the percentage of coverage area. We summarize here the magnetic properties of various Kagome materials with a variety of magnetic metal ions in Table 2. As can be seen, while the Fe^{3+} Kagome systems exhibit characteristics of frustrated low-temperature antiferromagnetism and occasional long-range antiferromagnetic order in the ground state,[6,45,61,62] vanadium (V^{3+}) jarosites are shown to exhibit ferromagnetism in the Kagome layers ($T_c \sim 33$ K).[68] On the other hand, chromium (Cr^{3+}) jarosite shows low-temperature antiferromagnetic behavior[72–76] while a Kagome compound of Co^{2+} [70] show strongly anisotropic high-spin Co(II) with appreciable spin–orbit coupling. A Cu^{2+} Kagome compound shows spin frustration,[46] while a Ni^{2+} sulfate with the Kagome structure[66] exhibits canted antiferromagnetism with magnetic polarization at low temperatures. An amine-templated mixed valent iron sulfate with the Kagome structure[48] becomes ferrimagnetic at low temperatures, although it shows some evidence for magnetic frustration. Interestingly, an organically templated Fe^{2+} sulfate with the Kagome structure also shows ferrimagnetic properties at low temperatures.[24,78] The question arises as to the cause for the marked differences in the magnetic properties of the V^{3+} Kagome compounds with the Fe^{3+} or Cr^{3+} and those with Fe^{2+}, mixed-valent Fe, Co^{2+}, Cu^{2+} and Ni^{2+}, although, all of them possess more or less the common Kagome network structure.

Since the Kagome network structure shares one spin between two adjacent triangles, as the basic unit, let us consider a two triangle structure with five spins, where one spin is common to both the triangles, as shown in Fig. 13. For a

Table 2 Magnetic properties of Kagome compounds with transition metal ions possessing different spins

Metal ion compound	S	θ_c/K	T_0/K	Magnetic properties
Cu^{2+}	0.5	−314	2	AFM interactions, no ordering[46]
Ni^{2+}	1	−60	9	AFM interactions, low-T hysteresis[66]
V^{3+}	1	+53	33	FM layers coupled antiferromagnetically[68]
Co^{2+}	1.5	−35	4	AFM interactions[70]
Cr^{3+}	1.5	−70	4	AFM interactions[72–76]
Fe^{2+} (perfect)	2	−75	19	AFM interactions, low-T hysteresis[24]
Fe^{2+} (distorted)	2		18	AFM interactions, low-T hysteresis[78]
Fe^{3+}	2.5	−820	65	AFM interactions, 3D ordering[45]
Mn^{2+}	2.5	−30	—	AFM interactions, no ordering[65]
Fe^{3+}/Fe^{2+}	2.5/2	−180	13	Ferrimagnet[48]

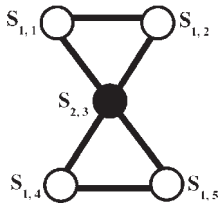

Fig. 13 Simplest corner-sharing two triangle structure. $S_{i,j}$ corresponds to spin s_i at site j.

general understanding, we consider spins $s1$ at the edges (numbered $S_{1,1}$, $S_{1,2}$, $S_{1,4}$ and $S_{1,5}$ in Fig. 13) of the two triangles and spin $s2$ as the corner shared (numbered $S_{2,3}$), so that there are four $s1$ spins and one $s2$ spin in this five-spin system. It is easy to solve this system exactly if we assume that the site spins interact *via* a nearest neighbor Heisenberg exchange Hamiltonian, which can be explicitly written as, $H = J[s_{1,1}\cdot s_{1,2} + s_{1,4}\cdot s_{1,5} + s_{2,3}\cdot(s_{1,1} + s_{1,2} + s_{1,4} + s_{1,5})]$, where each term is a dot product between two spin operators. We will consider the cases with $s1 = s2$ and $s1 \neq s2$ separately within this simple superexchange Hamiltonian. For $s1 = s2 = \frac{1}{2}$, the ground state is sixfold degenerate, with each doublet configuration of the shared spin giving rise to threefold degenerate states for each triangle. The ground-state magnetization is finite in each lattice point due to strong frustration. For $s1 = s2 = 1$, the ground state is threefold degenerate and is a singlet. There are three ways one can produce a singlet structure, and in each case, apart from the total magnetization, the magnetization in each of the edges as well as in the corner spin vanishes separately. Next we consider the cases with $s1 \neq s2$. There are two possibilities; each can be either an integer or a half-integer spin. For $s1 = \frac{1}{2}$ and $s2 = 1$, the ground state is a singlet and is threefold degenerate. The states are similar to the $s1 = s2 = 1$ case, although in this case, antiferromagnetic coupling in each edge is between the two spin-$\frac{1}{2}$ sites. For $s1 = \frac{1}{2}$ and $s2 = \frac{3}{2}$, the ground state is a doublet, with double degeneracy. Both the edges together form a triplet, which couples with the $Sz = \frac{1}{2}$ component of the spin $\frac{3}{2}$, and thereby removes the frustration completely in the corner-shared structure. By increasing the value of $s2$ further and keeping $s1 = \frac{1}{2}$ fixed, we get the same ferrimagnetic state with ground-state spin $S_G = s2–4s1$.

For a detailed theoretical study, we have considered 12- and 18-site Kagome lattices. They are shown in Fig. 14. Since experimentally there are examples of mixed-spin jarosite systems, we have considered a number of mixed spin together with unique site spin Kagome systems. In both cases, the integer as well as the half-integer spins are included.[79–82] The Hamiltonians correspond to antiferromagnetic exchanges between the spins connected by the solid lines (see Fig. 14). While the filled circles correspond to the $s1$ site spin, the empty circles have site spins $s2$. The site spins, $s1$ and $s2$, can be the same or different with integer (I) or half-integer (HI) values. Specifically, we consider the following four cases based on the above results for two-triangle systems: (a) $s1 = s2 = \frac{1}{2}$, (b) $s2 = \frac{1}{2}$ but $s1 = 1$, (c) $s1 = s2 = 1$, and (d) $s2 = 1$ and $s1 = \frac{1}{2}$. The periodic boundary conditions of the finite lattice systems ensure that these are small clusters of infinite two-dimensional Kagome structure. Note that the following results are with the

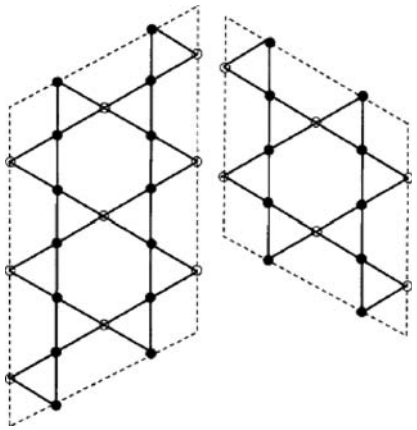

Fig. 14 Schematics of 12- and 18-site Kagome lattices. The solid lines represent the antiferromagnetic exchange interactions, J. The dashed line defines the periodic boundary conditions. The filled and empty circles represent the site spins $s1$ and $s2$, respectively.

Hamiltonian corresponding to an ideal Kagome lattice with localized site spins interacting *via* isotropic nearest-neighbor superexchange pathways. Later, we consider additional interaction terms corresponding to other energy scales due to lack of symmetry in the real systems. However, since most of these systems consist of 3d transition-metal narrow band ions, often the Heisenberg superexchange processes between nearest-neighbor localized moments set the dominant energy scale.

We have diagonalized the Hamiltonian matrix corresponding to the nearest-neighbor Heisenberg model for the above four systems with varying site spin $s1$, $s2$ values for both lattice sizes. Low-energy spectra in terms of total spin quantum number, S, can be obtained with the Hamiltonian matrix in a smallest S^z_{tot} sector, since every total spin has a projection in the smallest possible S^z_{tot} value. In Fig. 15, we compare and contrast the energy-level diagram as a function of total spin, S, for these four cases for an 18-site system. Although, we present results only for a fixed system size $N = 18$, for smaller spin values, we have verified that the low-energy spectrum remains qualitatively similar even for system sizes up to $N = 21$. For example, for $(\frac{1}{2}, \frac{1}{2})$ Kagome, the ground-state energies per site for (N sites) are −0.454 (12), −0.440 (15), −0.447 (18),

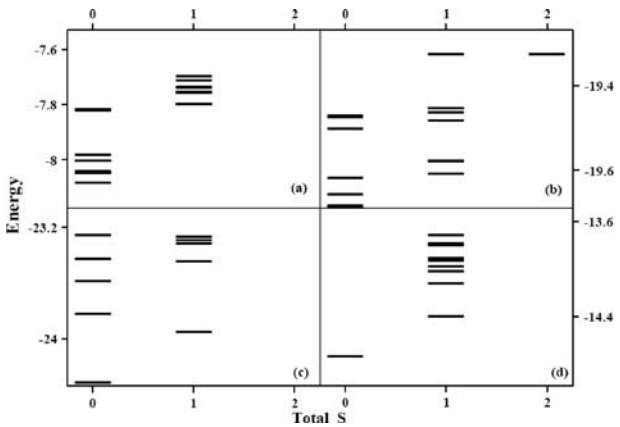

Fig. 15 Energy levels as a function of total spin S, for the ($s1$, $s2$) systems, for an 18-site cluster: (a) $(\frac{1}{2}, \frac{1}{2})$, (b) $(1, \frac{1}{2})$, (c) (1, 1) and (d) $(\frac{1}{2}, 1)$.

and −0.437 (21). Similarly, for (1, 1) and ($\frac{1}{2}$, 1), they are −1.468 (12) and −0.824 (12), −1.62 (15) and −0.81 (15), −1.34 (18) and −0.801 (18), and −1.39 (21) and −0.79 (21). Interestingly, the ground-state energy per site extrapolated to $N \rightarrow \infty$ for a spin-$\frac{1}{2}$ Kagome lattice was reported to be −0.434 by Zeng and Elser.[83] This shows that, for such small system sizes, the low-lying energy states are quite clearly defined, even for the smallest ($s1$, $s2$) values.

For cases (a) and (b) in Fig. 15, we find that the ground state is a non-degenerate singlet. The lowest excitations are to the singlet states for both cases although there are more numbers of excited singlet states very close to the ground state for case (a) than for case (b). Moreover, there exists a finite gap between the ground and the lowest magnetic states in both cases. In case (c), with $s1 = s2 = 1$, the ground state is a non-degenerate singlet and the lowest excited state is a magnetic triplet state. The low energy excitation spectrum consists of alternate singlet and triplet states and the system behaves more like a regular one-dimensional antiferromagnetic chain.[81,82] In fact, the ground state consists of a resonating valence bond (RVB) state with nearest-neighbor spins forming alternating singlet combinations and the lowest excitation involves energy cost (therefore the finite gap) due to disappearance of one of the singlets.[84] The situation becomes completely different for case (d). Although the ground state in this case is a singlet, the low-energy excitations are to the triplet states. Further, the number of low-energy triplet states increases rapidly with increase in system size. This is because in this case, the couplings between $s2$ and $s1$ spins become strongly antiferromagnetic forcing the $s1$–$s1$ couplings to be weakly ferromagnetic, since the $s1$ spins have smaller magnitude.[44] The in-plane and z-component spin–spin correlation functions are shown in Fig. 16.

Thus far, we have discussed the magnetic energy spectrum of various Kagome systems with only nearest neighbor Heisenberg interactions. However, in many of these systems, the magnetic ions are connected by anionic octahedral species through shared vertices, which remain most often tilted resulting in lowering of the overall hexagonal symmetry. For such geometry, another interaction term, known as the Dzyaloshinskii–Moriya (DM) Hamiltonian becomes important, in addition to the Heisenberg interaction. The DM Hamiltonian is of the type:

$$H_{\mathrm{DM}} = \sum_{ij} D_{ij}(S_i \times S_j)$$

Since this Hamiltonian is a vector, not only the spin-components become anisotropic, according to Moriya's rules,[85] but both the in-plane and the out-of-plane Dzyaloshinskii–Moriya (DM) vectors also become non-zero.[67,85–87] However, the out-of-plane coupling would not result in breaking the global rotational symmetry. The in-plane components (XY) of DM interactions, on the other hand, can induce canted spin moments in the out-of-plane directions (Z). Note that, inclusion of this term lowers the overall symmetry of the spin interactions in the system.

Since many of these systems show lowering of the crystal symmetry, we have analyzed the 12 site spin systems in terms of a Hamiltonian including XY components of DM interactions to the nearest-neighbor Heisenberg term discussed earlier. The Hamiltonian is:

$$H_{\mathrm{total}} = \sum_{\langle ij \rangle} JS_i \cdot S_j + \mathrm{d}_z(S_i^x S_j^y - S_j^x S_i^y)$$

where the DM part is written in terms of the spin components. By diagonalizing the Hamiltonian matrix, we obtain the energy spectrum and various ground state correlation functions. We find that with inclusion of the DM-term, the low lying excitations behave differently depending on the strength of out-of-plane (d_z) DM interactions. For our finite size ($\frac{1}{2}$, $\frac{1}{2}$) system, the number of singlets lying within the spin gap is finite, however, with an increase in the strength of DM interactions, this number reduces. In general, from the energy spectrum, we conclude that in cases where nonmagnetic states enter the spin-gap region, their number reduces with DM interactions, while for cases where a triplet is the lowest excitation, the DM interactions stabilize the triplet. This is because, with an increase in DM interaction strength, the nearest neighbour correlation between the z-components reduces, while the correlation between the in-plane component spins increases. This suggests that the spins become more and more tilted which enforces a finite spin moment for every magnetic ion triangle with the spins lying above and below the Kagome plane, resulting in magnetic polarizations. In fact, the magnitude of such a polarization depends crucially on the angle between the spins and the Kagome plane in the actual geometry and the resulting DM vector directions.

Although our model Hamiltonian calculations are for general Kagome systems, without consideration of details of each of the above experimental systems, the prediction of the model, however, confirms that within the nearest-neighbor superexchange processes and DM interactions, the variation of the magnitude of magnetic moments of ions plays a dominant role in governing the nature of the low-energy spectrum. Note that partially polarized magnetization or

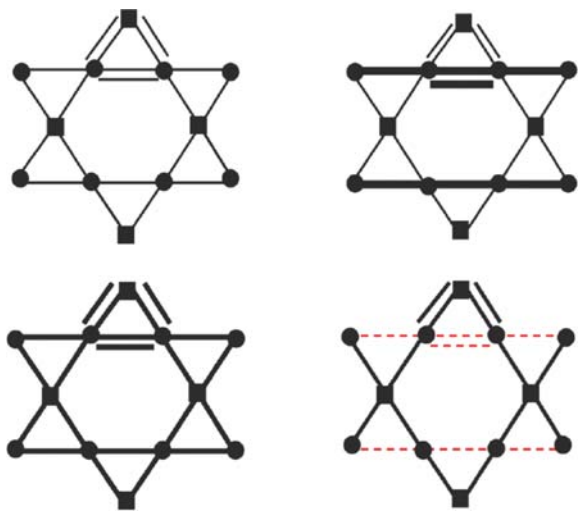

Fig. 16 z-Component spin–spin correlation functions (the additional lines in the upper triangle for each case are the in-plane correlation), where the four systems are in the following order: upper row from left ($\frac{1}{2}$, $\frac{1}{2}$) and (1, $\frac{1}{2}$); lower row from left (1, 1) and ($\frac{1}{2}$, 1). The thickness indicates the correlation strength. The solid line is for antiferromagnetic correlation and the dashed lines are for ferromagnetic correlations.

long-range magnetic order in the ground state may arise due to DM interactions determined by the magnetic anisotropy induced canted spin moments within a non-planar geometry. However, as has been mentioned, the DM-type interactions are generally present in systems without local inversion centers, which is reported to be the case for distorted Fe(III) Kagome systems. On the other hand, a V(III) Kagome layer is magnetically polarized due to geometrically favored ferromagnetic exchange couplings.[68] However, the half-integer spin systems without distortion, such as Fe^{3+} ($S = \frac{5}{2}$),[45] Cr^{3+} ($S = \frac{3}{2}$)[72–76] and Co^{2+} ($S = \frac{3}{2}$)[70] compounds, show low temperature antiferromagnetism, as our model predicts. A Cu^{2+} compound also has been reported to show strong manifestation of magnetic frustration, although at low temperature, due to small ferromagnetic interlayer coupling, the system develops some magnetic polarization.[46] Interestingly, two of the integer spin Kagome compounds reported so far, Fe^{2+} ($S = 2$)[77,78] and Ni^{2+} ($S = 1$),[66] show low-temperature magnetic polarization. Note that, removal of frustrations is crucial for the realization of a fully polarized state within a Kagome layer. The DM interactions, being weak in magnitude, can at best give small polarization at low temperature. In fact, the interplay between geometric factors, magnetic anisotropy, lattice disorder, and interplanar coupling and restrictive exchange processes in such a geometry governs the detailed nature of the low-energy and thereby the low-temperature properties of the Kagome network systems.

4. Summary and outlook

In conclusion, we have attempted to present the current state of knowledge in the area of frustrated Kagome network systems, emphasizing the structure and the magnetic properties of various Kagome systems with different magnetic ions. These systems are shown to exhibit magnetic phenomena ranging from long range order to spin glass and spin liquid behaviors. The experimental magnetic behaviors have been analyzed in terms of a generalized magnetic Hamiltonian with Heisenberg and inclusion of the Dzyaloshinskii–Moriya interactions arising due to local non-centrosymmetry in many of these systems. Our analysis shows that the role of the spin magnitudes of the magnetic ions is profound, giving rise to a variety of ground and excited state magnetic configurations and thereby varying the nature of the low-temperature thermodynamic properties, although the theoretical results described here are applicable for specialized isotropic Kagome lattices, with or without local non-centrosymmetry.

As indicated in the introduction, there also exist systems, called Keplerates, which are topologically similar to Kagome networks but occur in spherical shape with icosidodecahedral or cuboctahedral symmetry. Muller *et al.* have demonstrated that it is possible to build the spherically symmetrical structures with triangular or pentagonal units as building blocks.[35,88,89] Magnetic clusters with a $Mo_{72}M_{30}$ formula unit, where M = Fe, V, Cr, have been synthesized so far. Since these share similar topological features with Kagome networks, such a constrained geometry would be ideal to provide an alternate and rigorous understanding of the basic aspects of spin frustration-related magnetic properties and their relationship to the intrinsic magnetic moments of the magnetic ions.[90]

Another class of frustration-related systems are pyrochlore magnetic materials which are expected to show a range of phenomena including spin ice, spin-Peierls, heavy-fermion, high-T_c *etc.*[91–94] Particularly interesting are those systems where strong correlations might perturb a section of the system thereby giving the possibility of multiferroic behavior with or without ordering of spin transition. Interestingly, the change in ground state entropy during a transformation from a non-degenerate magnetically polarized state to a highly degenerate ground state upon application of field may lead to a large magnetocaloric effect. Such an adiabatic demagnetization may thus be useful in prospective refrigerant materials at low temperature which are widely considered for space applications.[95]

There are issues of quantum fluctuations, long-range exchange, chiral vectors and microscopic disorder which need to be understood in a more general sense. We may hope that the current experimental and theoretical studies of multidimensional frustrated systems will lead to a deeper understanding of frustration-related effects in rare-earth and transition metal magnetic systems in quasi-two and three dimensions. Such an understanding might be relevant to as yet to be discovered systems where various competing interactions may be useful for a range of applications in thermal, mechanical, optical, electrical and magnetic phenomena. We expect that discrete and collective behavior of these and related materials will continue to capture the attention of solid-state and materials chemists and physicists alike.

Notes and references

1 L. Pauling, *J. Am. Chem. Soc.*, 1935, **57**, 2680.
2 W. F. Giauque and M. Ashley, *Phys. Rev.*, 1933, **43**, 81.
3 W. F. Giauque and J. W. Stout, *J. Am. Chem. Soc.*, 1936, **58**, 1144.
4 J. B. Goodenough, *Magnetism and the Chemical Bond*, Wiley-Interscience, New York, 1963.
5 A. P. Ramirez, *Annu. Rev. Mater. Sci.*, 1994, **24**, 453.
6 J. E. Greedan, *J. Mater. Chem.*, 2001, **11**, 37.
7 A. P. Ramirez, in *Handbook on Magnetic Materials*, ed. K. J. H. Busch, Elsevier Science, Amsterdam, 2001, vol. 13, pp. 423.
8 K. Binder and A. P. Young, *Rev. Mod. Phys.*, 1986, **58**, 801.
9 R. de Pape and G. Ferey, *Mater. Res. Bull.*, 1986, **21**, 971.
10 A. B. Harris, C. Kallin and A. J. Berlinsky, *Phys. Rev. B: Condens. Matter Mater. Phys.*, 1992, **45**, 2899.
11 O. Kahn, *Molecular Magnetism*, Wiley-VCH, NY, 1993.
12 J. Renaudin, G. Ferey, M. Lahlou-Mimi, J. M. Greneche, Y. Mary and A. Kozac, *J. Magn. Magn. Mater.*, 1991, **92**, 381.
13 C. N. R. Rao and B. Raveau, *Transition Metal Oxides*, VCH Publishers, NY, 1995.
14 S. K. Pati, S. Ramasesha and D. Sen, in *Magnetism: Molecules to Materials IV*, ed. J. S. Miller and M. Drillon, Wiley-VCH, Weinheim, 2002, pp. 119–171,.
15 P. Day, *Molecules into Materials: Case Studies in Materials Chemistry – Mixed Valency, Magnetism and Superconductivity*, World Scientific, Singapore, 2007.
16 S. K. Pati, *Phys. Rev. B: Condens. Matter Mater. Phys.*, 2003, **67**, 184411.
17 D. Parihari and S. K. Pati, *Phys. Rev. B: Condens. Matter Mater. Phys.*, 2004, **70**, 180403(R).
18 S. Soulette, M. Drillon, P. Rabu and S. K. Pati, *Phys. Rev. B: Condens. Matter Mater. Phys.*, 2004, **70**, 054410.
19 L. Capogna, M. Mayr, P. Horsch, M. Raichle, R. K. Kremer, M. Sofin, A. Maljuk, M. Jansen and B. Keimer, *Phys. Rev. B: Condens. Matter Mater. Phys.*, 2005, **71**, 140402.
20 A. C. Mclaughlin, J. A. McAllister, L. D. Stout and J. P. Attfield, *Phys. Rev. B: Condens. Matter Mater. Phys.*, 2002, **65**, 172506.
21 A. Koga and N. Kawakami, *Phys. Rev. B: Condens. Matter Mater. Phys.*, 2001, **63**, 144432.
22 L. Capriotti, A. E. Trumper and S. Sorellla, *Phys. Rev. Lett.*, 1999, **82**, 3899.

23 S. Nakatsuji, Y. Nambu, H. Tonomura, O. Sakai, S. Jonas, C. Broholm, H. Tsunetsugu, Y. Qiu and Y. Maeno, *Science*, 2005, **309**, 1697.
24 C. N. R. Rao, E. V. Sampathkumaran, R. Nagarajan, G. Paul, J. N. Behera and A. Choudhury, *Chem. Mater.*, 2004, **16**, 1441.
25 D. G. Nocera, B. M. Barlett, D. Grohol, D. Papoutsakis and M. P. Shores, *Chem.–Eur. J.*, 2004, **10**, 3850.
26 S. T. Bramwell and M. J. P. Gingras, *Science*, 2001, **294**, 1495.
27 R. R. P. Singh and D. A. Huse, *Phys. Rev. Lett.*, 1992, **68**, 1766.
28 F. Nori, E. Gagliano and S. Bacci, *Phys. Rev. Lett.*, 1992, **68**, 240.
29 A. S. Wills, V. Dupuis, E. Vincent, J. Hammann and R. Calemczuk, *Phys. Rev. B: Condens. Matter Mater. Phys.*, 2000, **62**, R9264.
30 T. Kato, K. Hondou and K. Iio, *J. Magn. Magn. Mater.*, 1998, **177**, 591.
31 T. Hasegawa, M. Inui, K. Hondou, Y. Fujiwara, T. Kato and K. Iio, *J. Alloys Compd.*, 2004, **364**, 199.
32 N. Oba, C. Michioka, M. Kato, K. Yoshimura and Ko Mibu, *J. Phys. Chem. Solids*, 2005, **66**, 1438.
33 X. Obradors, A. Labarta, A. Isalgué, J. Tejada, J. Rodriguez and M. Pernet, *Solid State Commun.*, 1988, **65**, 189; F. Ladieu, F. Bert, V. Dupuis, E. Vincent and J. Hammann, *J. Phys.: Condens. Matter*, 2004, **16**, 5735.
34 N. Rogado, G. Lawes, D. A. Huse, A. P. Ramirez and R. J. Cava, *Solid State Commun.*, 2002, **124**, 229; N. Rogado, M. K. Haas, G. Lawes, D. A. Huse, A. P. Ramirez and R. J. Cava, *J. Phys.: Condens. Matter*, 2003, **15**, 907.
35 A. M. Todea, A. Merca, H. Bogge, J. Slageren, M. Dressel, L. Engelhardt, M. Luban, T. Glaser, M. Henry and A. Muller, *Angew. Chem., Int. Ed.*, 2007, **119**, 6218.
36 D. A. V. Griend, S. Boudin, V. Caignaert, K. Poeppelmeier, Y. Wang, V. P. Dravid, M. Azuma, M. Takano, Z. Ho and J. D. Jorgensen, *J. Am. Chem. Soc.*, 1999, **121**, 4787.
37 M. D. Nunez-Regueiro, C. Lacroix and B. Canals, *Phys. Rev. B: Condens. Matter Mater. Phys.*, 1996, **54**, 736.
38 Y. R. Wang, *Phys. Rev. B: Condens. Matter Mater. Phys.*, 1992, **45**, 12608, and references cited therein.
39 R. R. P. Singh and D. A. Huse, *Phys. Rev. Lett.*, 1992, **68**, 1766.
40 V. O. Cheranovski, T. G. Schmalz and D. J. Klein, *J. Chem. Phys.*, 1994, **101**, 5841.
41 S. K. Pati and R. R. P. Singh, *Phys. Rev. B: Condens. Matter Mater. Phys.*, 1999, **60**, 7695.
42 F. Mila, *Phys. Rev. Lett.*, 1998, **81**, 2356.
43 C. Waldtmann, H. U. Everts, B. Bernu, P. Sindzingre, C. Lhuillier, P. Lecheminant and L. Pierre, *Eur. Phys. J. B*, 1998, **2**, 501.
44 S. K. Pati and C. N. R. Rao, *J. Chem. Phys.*, 2005, **123**, 234703.
45 B. M. Bartlett and D. G. Nocera, *J. Am. Chem. Soc.*, 2005, **127**, 8985.
46 M. P. Shores, E. A. Nytko, B. M. Bartlett and D. G. Nocera, *J. Am. Chem. Soc.*, 2005, **127**, 13462.
47 E. A. Nytko, J. S. Helton, P. Muller and D. G. Nocera, *J. Am. Chem. Soc.*, 2008, **130**, 2922.
48 C. N. R. Rao, G. Paul, A. Choudhury, E. V. Sampathkumaran, A. K. Raychaudhuri, S. Ramasesha and I. Rudra, *Phys. Rev. B: Condens. Matter Mater. Phys.*, 2003, **67**, 134425.
49 I. D. Brown and D. Altermatt, *Acta Crystallogr., Sect. B: Struct. Sci.*, 1985, **41**, 244.
50 (*a*) J. Selbin, L. H. Holmes and S. P. McGlynn, *J. Inorg. Nucl. Chem.*, 1963, **25**, 1359; (*b*) K. Nakamoto, *Infrared and Raman Spectra of Inorganic and Coordination Compounds*, Wiley, New York, 1978.
51 (*a*) J. E. Dutrizac and S. Kaiman, *Can. Mineral.*, 1976, **14**, 151; (*b*) F. C. Hawthrone, S. V. Krivovichev and P. C. Burns, *Rev. Mineral. Geochem.*, 2000, **40**, 1.
52 N. E. Brese and M. O'Keeffe, *Acta Crystallogr., Sect. B: Struct. Sci.*, 1991, **47**, 192.
53 N. N. Greenwood and T. C. Gibb, *Mössbauer Spectroscopy*, Chapman and Hall, London, 1971.
54 G. M. Sheldrick, *SHELXS-86, Computer Program For Crystal Structure Determination*, University of Gottingen, Gottingen, Germany, 1986.
55 G. M. Sheldrick, *SHELXS-PLUS, Computer Program For Crystal Structure Solution And Refinement*, University of Gottingen, Gottingen, Germany, 1993.
56 A. S. Wills and A. Harrison, *J. Chem. Soc., Faraday Trans.*, 1996, **92**, 2161.
57 A. S. Wills, A. Harrison, C. Ritter and R. I. Smith, *Phys. Rev. B: Condens. Matter Mater. Phys.*, 2000, **61**, 6156.
58 A. Harrison, A. S. Wills and C. Ritter, *Phys. B (Amsterdam, Neth.)*, 1998, **241–243**, 6156.
59 A. S. Wills, A. Harrison, S. A. M. Mentink, T. E. Mason and Z. Tun, *Europhys. Lett.*, 1998, **42**, 325.
60 G. S. Oakley, D. Visser, J. Frunzke, K. H. Andersen, A. S. Wills and A. Harrison, *Phys. B (Amsterdam, Neth.)*, 1999, **267–268**, 142.
61 D. Grohol and D. G. Nocera, *J. Am. Chem. Soc.*, 2002, **124**, 2640.
62 D. Grohol, D. G. Nocera and D. Papoutsakis, *Phys. Rev. B: Condens. Matter Mater. Phys.*, 2003, **67**, 064401.
63 T. Inami, S. Maegawa and M. Takano, *J. Magn. Magn. Mater.*, 1998, **177–181**, 752.
64 T. Inami, M. Nishiyama, S. Maegawa and Y. Oka, *Phys. Rev. B: Condens. Matter Mater. Phys.*, 2000, **61**, 12181.
65 J. N. Behera and C. N. R. Rao, *Dalton Trans.*, 2007, 669.
66 J. N. Behera and C. N. R. Rao, *J. Am. Chem. Soc.*, 2006, **128**, 9334.
67 J. N. Behera, A. Sundaresan, S. K. Pati and C. N. R. Rao, *ChemPhysChem*, 2007, **8**, 217.
68 D. Grohol, D. Papoutsakis and D. G. Nocera, *Angew. Chem., Int. Ed.*, 2001, **40**, 1519.
69 D. Papoutsakis, D. Grohol and D. G. Nocera, *J. Am. Chem. Soc.*, 2002, **124**, 2647.
70 J. N. Behera, G. Paul, A. Choudhury and C. N. R. Rao, *Chem. Commun.*, 2004, 456.
71 C. Livage, C. Egger and G. Ferey, *Chem. Mater.*, 1999, **11**, 1546.
72 C. Broholm, G. Aeppli, G. P. Espinosa and A. S. Cooper, *Phys. Rev. Lett.*, 1990, **65**, 3173.
73 S. H. Lee, C. Broholm, G. Aeppli, T. G. Perring, B. Hessen and A. Taylor, *Phys. Rev. Lett.*, 1996, **76**, 4424.
74 A. Keren, P. Mendels, M. Horvatic, F. Ferrer, Y. J. Uemura, M. Mekata and T. Asano, *Phys. Rev. B: Condens. Matter Mater. Phys.*, 1998, **57**, 10745.
75 A. Keren, Y. J. Uemura, G. Luke, P. Mendels, M. Mekata and T. Asano, *Phys. Rev. Lett.*, 2000, **84**, 3450.
76 A. P. Ramirez, G. P. Espinosa and A. S. Cooper, *Phys. Rev. Lett.*, 1990, **64**, 2070.
77 C. N. R. Rao, E. V. Sampathkumaran, R. Nagarajan, G. Paul, J. N. Behera and A. Choudhury, *Chem. Mater.*, 2004, **16**, 1441.
78 G. Paul, A. Choudhury and C. N. R. Rao, *Chem. Commun.*, 2002, 1904.
79 R. Chitra, S. K. Pati, D. Sen, H. R. Krishnamurthy and S. Ramasesha, *Phys. Rev. B: Condens. Matter Mater. Phys.*, 1995, **52**, 6581.
80 S. Mohakud, S. K. Pati and S. Miyashita, *Phys. Rev. B: Condens. Matter Mater. Phys.*, 2007, **76**, 014435.
81 S. K. Pati, R. Chitra, D. Sen, H. R. Krishnamurthy and S. Ramasesha, *Europhys. Lett.*, 1996, **33**, 707.
82 S. K. Pati, R. Chitra, D. Sen, S. Ramasesha and H. R. Krishnamurthy, *J. Phys.: Condens. Matter*, 1997, **9**, 219.
83 C. Zeng and V. Elser, *Phys. Rev. B: Condens. Matter Mater. Phys.*, 1990, **42**, 8436.
84 K. Hida, *J. Phys. Soc. Jpn.*, 2000, **69**, 4003.
85 T. Moriya, *Phys. Rev.*, 1960, **120**, 91.
86 M. Elhajal, B. Canals and C. Lacroix, *Phys. Rev. B: Condens. Matter Mater. Phys.*, 2002, **66**, 014422.
87 S. Mohakud, K. Hijii, S. Miyashita and S. K. Pati, unpublished.
88 A. Muller, M. Luban, C. Shroder, R. Modler, P. Kogerler, M. Axenovich, J. Schnack, P. Canfield, S. Bud'ko and N. Harrison, *ChemPhysChem*, 2001, **2**, 517.
89 A. Muller, A. M. Todea, J. Slageren, M. Dressel, H. Bogge, M. Schmidtmann, M. Luban, L. Engelhardt and M. Rusu, *Angew. Chem., Int. Ed.*, 2005, **44**, 3857.
90 I. Rousochatzakis, A. M. Lauchli and F. Mila, *Phys. Rev. B: Condens. Matter Mater. Phys.*, 2008, **77**, 094420.
91 M. A. Subramanian, G. Aravamudan and G. V. Subba Rao, *Prog. Solid State Chem.*, 1983, **15**, 55.
92 M. J. Harris and M. P. Zinkin, *Mod. Phys. Lett. B*, 1996, **10** 417.
93 M. Enjalran, M. J. P. Gingras, Y.-J. Kao, A. D. Maestro and H. R. Molavian, *J. Phys.: Condens. Matter*, 2004, **16**, S673.
94 R. Moessner and A. R. Ramirez, *Phys. Today*, 2006, **59**, 24.
95 S. Maekawa, T. Tohyama, S. E. Barnes, S. Ishihara, W. Koshibae and G. Khaliullin, *Physics of Transition Metal Oxides*, Springer-Verlag, Berlin, 2004.